



STRUCTURE AND PROPERTIES OF SEVERAL STEELS
PRODUCED BY CONTROLLED SOLIDIFICATION PROCESSES

MOHAMED A. TAHA

Professor, Department of Mechanical Design and
Production Engineering, Ain Shams University,
Abaseia, Cairo - EGYPT.

ABSTRACT

Controlled solidification has considered a great attention in the last decade with the engineering aim of developing structures with improved properties and performance characteristics. Fundamental and applied research work in this field has led to the finding out of new processes which produce improved or novel structures. Steady state directional solidification (DS) and stir or rheo-casting (RC) are two examples of these processes, which have been applied in this work on several types of steel. The improvements gained in structure, segregation and mechanical properties, due to the application of these processes compared to the conventional casting (CC) are briefly presented in this paper referring to author's work.

In DS, plain carbon, low alloyed Mn-Ni, highly alloyed Mn, Mn-Ni and Cr and low carbon steels have been considered. Generally, the structure of these steels has dendrites aligned in the heat flow direction. A rod-like dendrite shape is obtained at high G/R values (G is the temperature gradient and R is the growth rate) while secondary and tertiary dendrite arms appear as G/R values decreases. Measurements of dendrite arm spacings show that they are functions of $R^{-n}G^{-m}$. Such relationship is useful in controlling the structure and hence the properties. Mechanical testing of some castings indicates high tensile properties for the rod-like DS structure which is even higher than that of the forged structure for the same material.

In RC, a novel structure with nearly spherical primary particles is obtained for the carbon and stainless steels used. Homogene-



INTRODUCTION

Increasing attention is being directed towards the control of solidification structure resulted from the casting process. Control of the as cast structure means the control of different segregation aspects which are generally formed upon solidification as micro and macro-segregations and inclusions, precipitates and hence the control of all as-cast properties.^(1,2)

During the last decade, a lot of research work has made emphasis towards the improvement of casting properties by applying some novel controlled solidification processes which result in well controlled and defined structure.^(1,3,4)

Steel castings have in most cases dendritic structure. Their properties are directly and strongly affected by the dendrite arm spacings.^(1,2) The dendrite arm spacings can be controlled by the solidification parameters which are growth rate and temperature gradient as well as steel composition.⁽⁵⁻⁷⁾ such parameters can be separately controlled in the unidirectional solidification process (DS).⁽¹⁻¹⁰⁾ In this controlled solidification process, the structure consists of a composite-like aligned one which results in improved mechanical properties in the heat flow direction.^(6,8-10) In the case of steel castings, application of the process produces arrays of dendrites with well defined arm spacings.^(1,2,5-7)

Another process in which the structure produced is a homogeneous nondendritic one, is the stir or rheo-casting (RC)^(3,4,11-20)

In this process, the turbulent flow due to stirring of the solidifying alloy, leads to the formation of the primary particles with nearly rounded shape instead of the dendritic one.⁽¹¹⁻²⁰⁾

The process have shown many promising properties as the structure, composition and mechanical properties are homogeneous throughout the casting.^(11,16-20) The process show a possibility

for easier steel die casting process due to pouring from a temperature below the liquidus.⁽¹³⁻¹⁵⁾ However, its practical appl-

MP-10 113



SECOND A.M.E. CONFERENCE

6 - 8 May 1986 , Cairo

5

ous structure in all casting parts as well as lack of macrosegregation and flat microconcentration profile are obtained. The tensile and compression properties are also homogeneous in the RC castings. It is found that the RC structure exhibits compressive strength and ductility several times those in tension.



UNIDIRECTIONAL SOLIDIFICATION

Materials and Experimental Procedures

The type, composition and solidification range and characteristics of steels investigated are given in table:1. (A) is a plain carbon, (B) is a low alloyed Mn-Ni, (C) and (D) are highly alloyed austenitic Mn and Mn-Ni respectively, (E) is a highly alloyed ferritic-Cr and (W) and (X) are low carbon steels with too low S content. The liquidus and solidus temperatures T_L and T_S , were determined by differential thermal analysis.⁽⁵⁻⁷⁾

Steady state unidirectional solidification apparatus used is shown schematically in Fig.1. Cylindrical casting 14 mm in diameter and about 170 to 200 mm long were solidified by withdrawing an alumina crucible containing steel downwards from a high temperature tannan furnace through a water cooled copper head. The growth rate (R) and temperature gradient (G) varied between 30 to 510 mm.h⁻¹ and 9 to 250 K.cm⁻¹ respectively. R is taken as the specimen withdrawal speed. G is calculated from the temperature - distance plots recorded during the experiment as $T_L - T_S$ divided by d, where d is the length of mushy zone. More details are found elsewhere.⁽⁵⁻⁷⁾

Microstructure Observations

Microstructure was observed in the heat flow direction and normal to it. In some cases,⁽⁶⁾ the structure was revealed after a suitable heat treatment process. The microstructure of the unidirectionally solidified steels investigated consists of arrayed dendrites in the direction of heat flow (longitudinal direction of the cylindrical casting). Typical photomicrographs of this microstructure , in the longitudinal and transverse directions, for the different steels are shown in Fig.2. These photomicrographs represent different solidification conditions, i.e. different combinations of G and R. Generally, the dendritic morphology shows a great dependence on R, G and steel composition. At increasing R and decreasing G, the dendrites become more branched. Fig.2(a) shows how the structure of steel (B) is changed



Table 1 : Composition, solidification range and characteristics of unidirectionally solidified steels.

Steel Name, Type	Chemical Composition, wt%	Solidification Range		Solidification Characteristics
		T _L , °C	T _S , °C	
A) Plain Carbon	0.57 C, 0.57 Mn, 0.11 Si, 0.005 P, 0.060 S, 0.043 Al.	1493	1430	
B) Low Alloyed Mn-Ni	0.60 C, 2.0 Mn, 1.00 Ni.	1492	1411	
C) Highly All- oyed Mn	0.64 C, 27.7 Mn, 0.042 Si, 0.007 P, 0.013 S, 0.075 Al.	1402	1296	Solidifies as austenite
D) Higly All- oyed Mn-Ni	0.63 C, 10.0 Mn, 0.009 Si, 14.9 Ni, 0.009 P, 0.008 S.	1400	1307	Solidifies as austenite
E) Highly All- oyed Cr	0.68 C, 1.1 Si, 28.3 Cr.	1448	1272	Ferrite primary phase
F) Low Carbon	0.15 C, 1.44 Mn, 0.37 Si, 0.012 P, 0.0014 S.	1505	1454	{ Ferrite primary phase, Peritectic transform- ation to austenite
G) Low Carbon	0.093 C, 1.3 Mn, 0.041 Si, 0.016 P, 0.0012 S.	1508	1466	

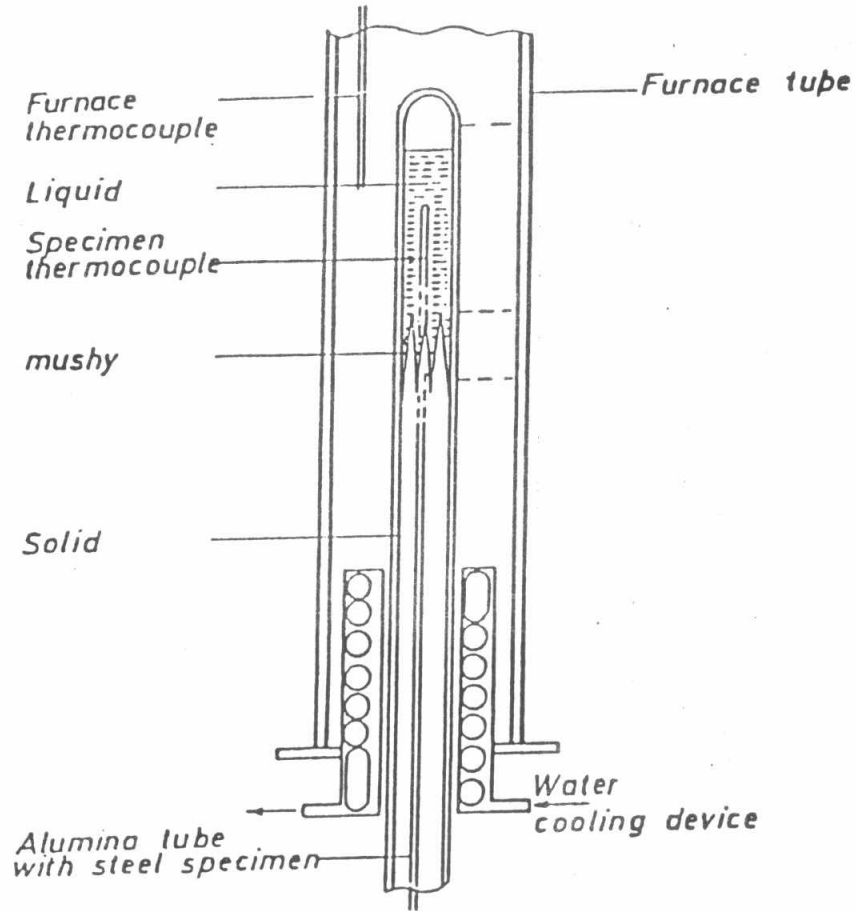


Fig.1 : Apparatus used for unidirectional solidification of steel.



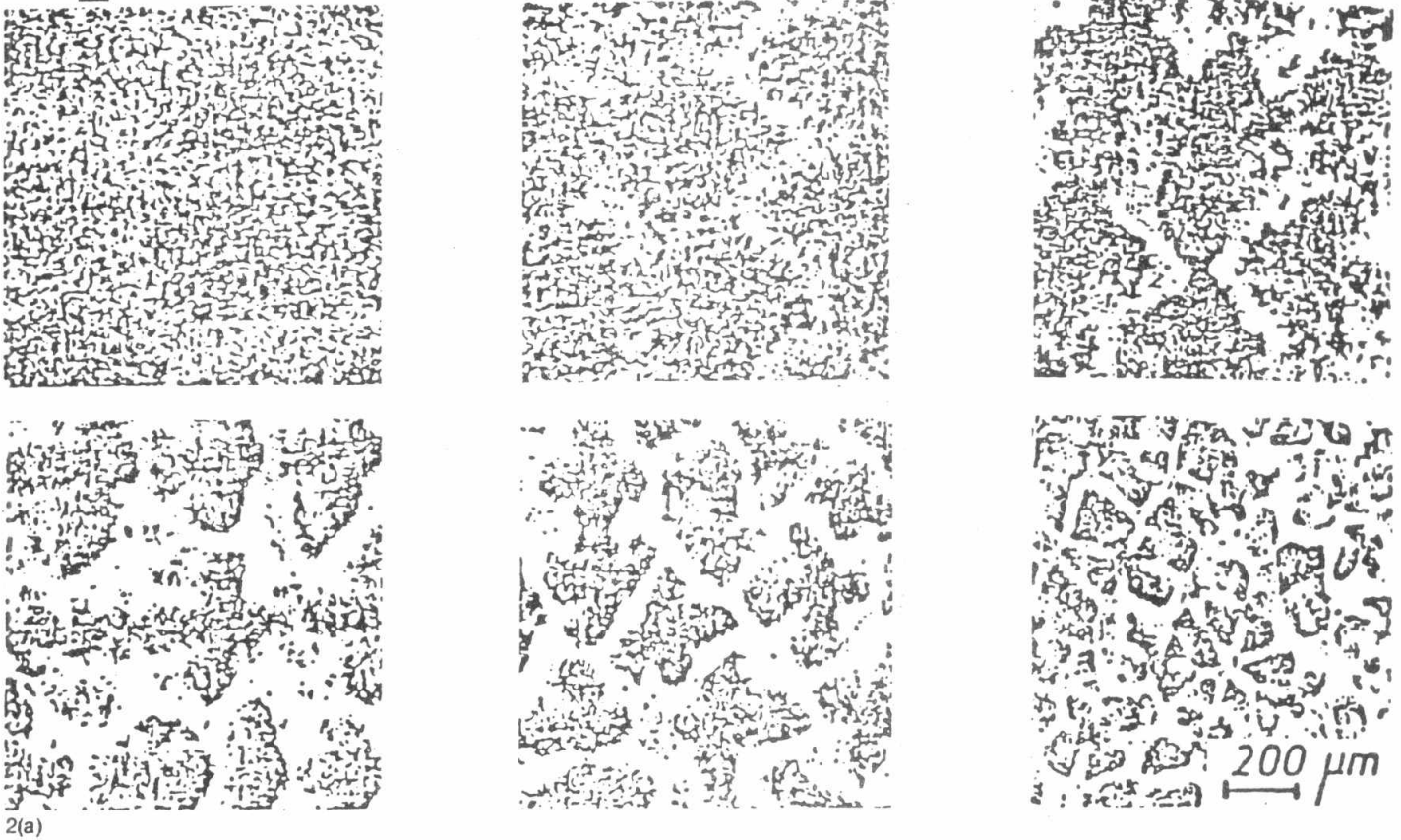
greatly with varying R, keeping G constant. At low R, the dendrites in the transverse section are nearly round in shape. Longitudinal section shows in this case no secondary arms, i.e. the dendrites are rod-like in shape. Secondary arms are observed at G/R lower than $23 \times 10^2 \text{ K.s.mm}^{-1}$, while tertiary arms appeared at G/R lower than $9 \times 10^2 \text{ K.s.mm}^{-1}$.

The dendritic morphology of the austenitic steel (C) is shown in Fig.2(b) for two different conditions: i) low R combined with high G and ii) high R combined with very low G. Although that the calculated local solidification time is almost the same for both conditions, the structure changed greatly due to the variation of R and G. In the first case, the dendrites are rod-like, while in the second case, secondary and tertiary arms are developed. The micrographs of the other austenitic steel (D), shown in Fig.2(c), gives another example of two different conditions where R is constant (510 mm.h^{-1}) and G is variable: i) 23 K.cm^{-1} and ii) 137 K.cm^{-1} . Again, at low G secondary and tertiary arms are observed while at high G there is a trend for the disappearance of such arms. However, the secondary arms in Fig. 2(c-ii), show a caplike shape as a transition between branched and rod-like dendrites.⁽⁵⁾

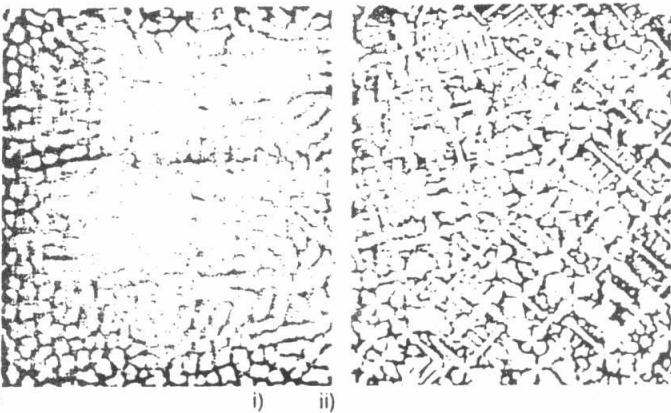
The ferritic steel (E), Fig.2(d), shows different behavior where the dendrites are branched at all solidification conditions used.

The structure of low carbon steels are shown in Fig.2(e) and 2(f) for steel (W) and steel (X) respectively. The dependence of the morphology on R and G is also clear in this case. At low R and high G, the dendrites exhibited perfect shape with cross-like primary arms. In steel (X) with lower C%, rod-like shape was obtained under these conditions. With increasing R and decreasing G, the dendrites become more branched with elongated shape in the transverse section at extremely high R and low G.

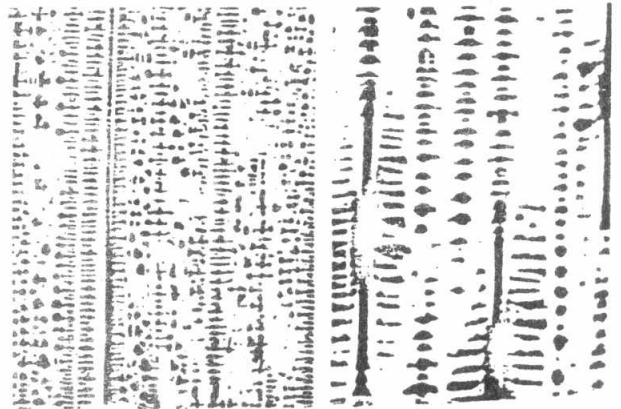
From the above observations, it seems that the influence of R and G on the dendritic morphology is similar for all types and compositions of steels investigated.



2(a)



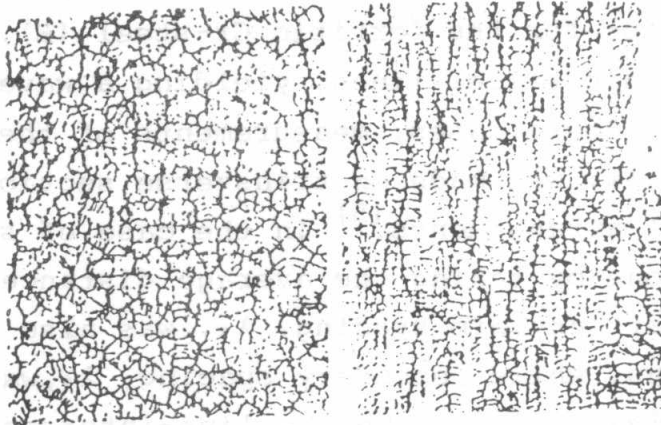
2(h)



2(c)

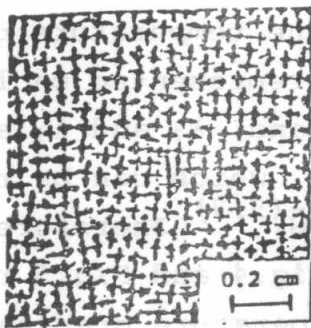
Figure 2. Typical photomicrographs of the microstructure obtained for different unidirectionally solidified steels:

- (a) low alloyed Mn-Ni steel (B), transverse section at $R = 15, 30, 60, 120, 200$ and 510 mm.h^{-1} , $G = 130 \text{ K.cm}^{-1}$.
- (b) austenitic steel (C), transverse section at: i) $G = 700 \text{ K.cm}^{-1}$, $R = 30 \text{ mm.h}^{-1}$ and ii) $G = 29 \text{ K.cm}^{-1}$, $R = 510 \text{ mm.h}^{-1}$, (Ref: 5).
- (c) austenitic steel (D), transverse and longitudinal sections at: i) $G = 23 \text{ K.cm}^{-1}$ and ii) $G = 137 \text{ K.cm}^{-1}$, $R = 510 \text{ mm.h}^{-1}$, (Ref: 5).
- (d) ferritic steel (E), transverse and longitudinal sections at $G = 198 \text{ K.cm}^{-1}$ and $R = 30 \text{ mm.h}^{-1}$, (Ref: 5).
- (e) low carbon steel (W), transverse sections at: i) $G = 12.6 \text{ K.cm}^{-1}$, $R = 510 \text{ mm.h}^{-1}$ and ii) $G = 19.2 \text{ K.cm}^{-1}$, $R = 120 \text{ mm.h}^{-1}$.



2(d)

0.1 cm

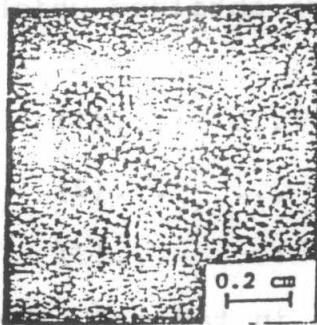


i)



ii)

2(e)



i)



ii)

2(f)



Dendrite Arm Spacings

In all cases, except for the ferritic Cr-steel (E), the primary arms are aligned on parallel lines, yielding a wave-like segregation pattern. In these cases, measurements of the average primary arm spacing, λ_1 , was made on transverse sections using the model of hexagonal arrangements.⁽⁵⁾ In the case of steel (E), measurement was done by taking the average distance between nearest neighbors. Tertiary arm spacing, λ_3 , was also measured on transverse sections, while secondary spacing, λ_2 , was measured on longitudinal sections, both using the line-intersect method.

λ_1 , is controlled by the phenomenon occurring at the dendrite tip. Therefore, it is controlled by the temperature gradient at the liquidus, G_L . λ_1 vs. G_L data are represented on log-log plots as shown in Fig.3. On the other hand, λ_2 and λ_3 are controlled by the local solidification time, which can be represented by the average temperature gradient, \bar{G} .^(5,7) Therefore, they are correlated with \bar{G} as represented in Fig.4 and Fig.5 respectively. In the case of steel (B), the temperature gradient was kept constant and R was varied. λ_1 is plotted vs. R as shown in Fig.6. In all these plots, straight lines are obtained which indicate the following relationships:

$$\lambda_1 = C_1 \cdot R^{-n_1} \cdot G_L^{-m_1} \quad \dots \quad (1)$$

$$\lambda_2 = C_2 \cdot R^{-n_2} \cdot \bar{G}^{-m_2} \quad \dots \quad (2)$$

$$\lambda_3 = C_3 \cdot R^{-n_3} \cdot \bar{G}^{-m_3} \quad \dots \quad (3)$$

The values of the exponents are given in table:2. The exponent n_1 is constant and does not depend on R, for all types of steel, except for the austenitic ones (C) and (D). However, it seems that this exponent is not necessary independent of R, as it is found to increase with increasing R for these types of austenitic steels. In this case, an average value for the exponent is calculated and is given in table:2.

The exponents n_2 and n_3 are found to be independent of R. The exponents m_1 , m_2 and m_3 are independent of G_L and \bar{G} .

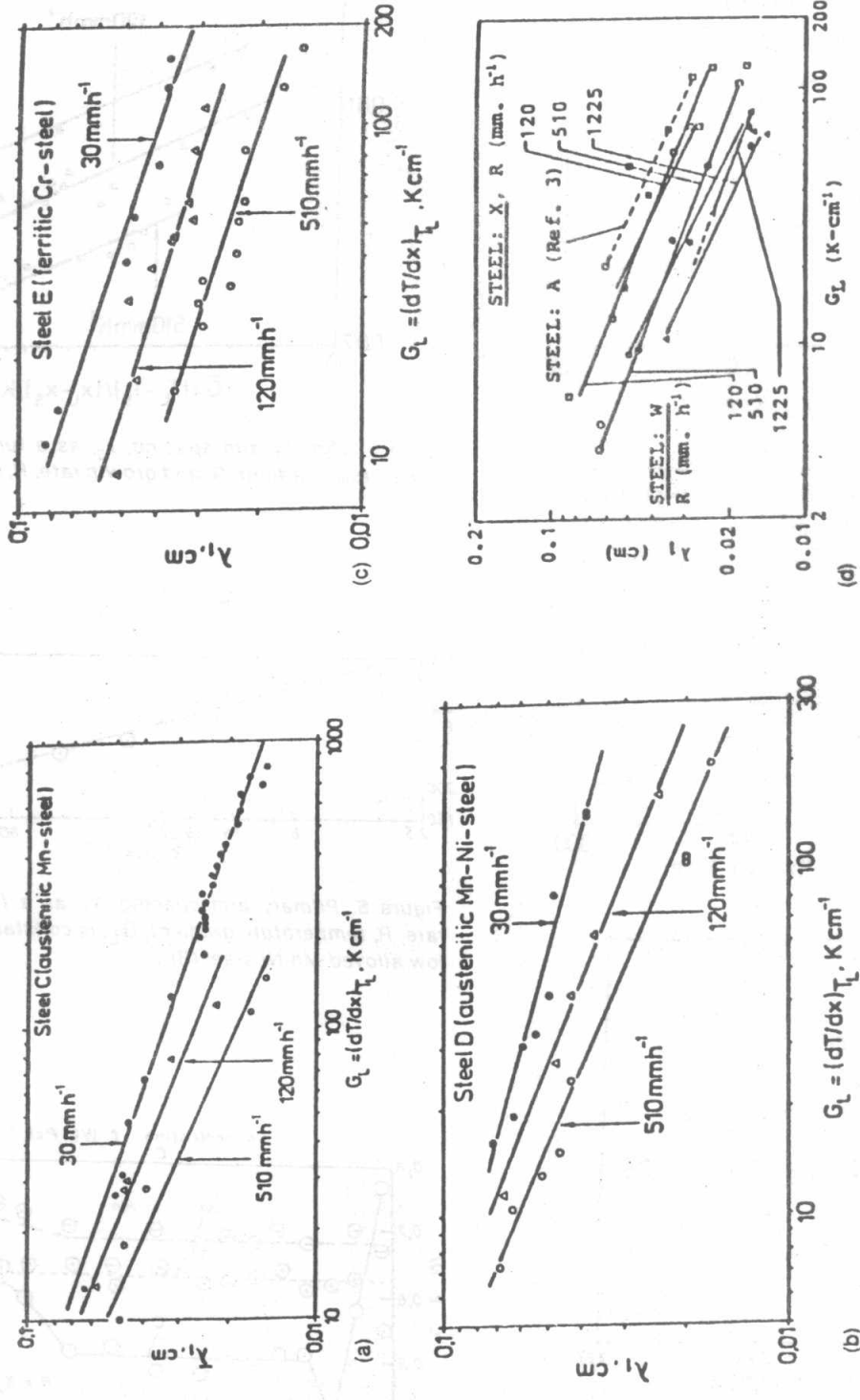


Figure 3. Primary dendrite arm spacing, λ_1 , as a function of temperature gradient at the liquidus, G_L , and growth rate, R .

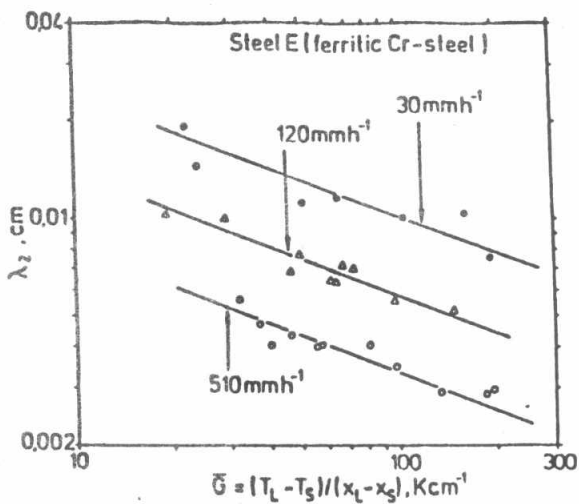
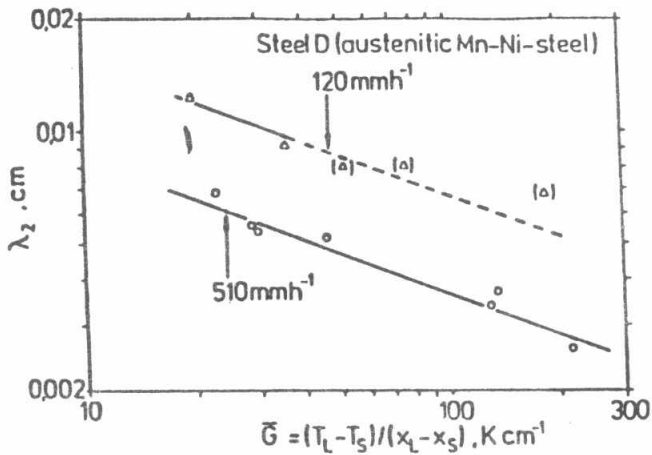
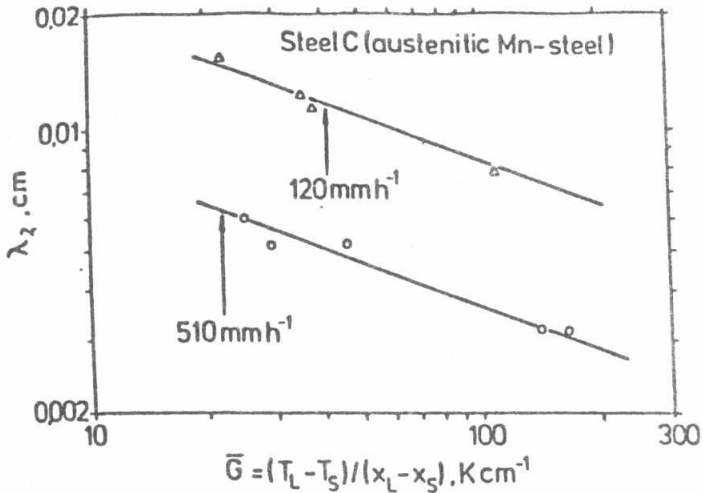


Figure 4. Secondary arm spacing, λ_2 , as a function of average temperature gradient, G , and growth rate, R :

- (a) austenitic steel (C),
- (b) austenitic steel (D) and
- (c) ferritic steel (E).

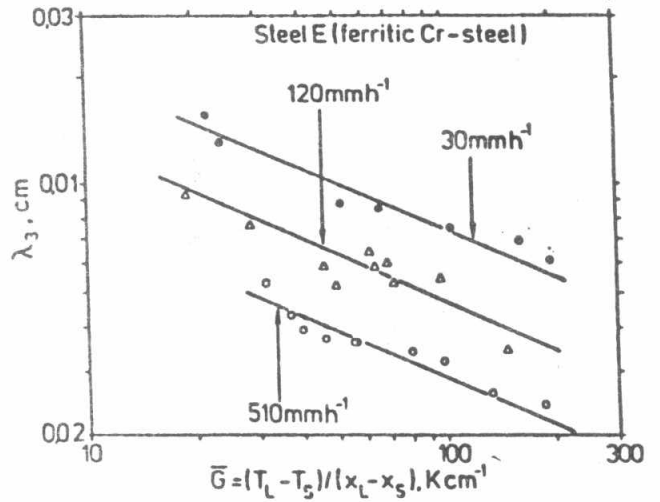


Figure 5. Tertiary arm spacing, λ_3 , as a function of average temperature gradient, G , and growth rate, R , in ferritic steel (E).

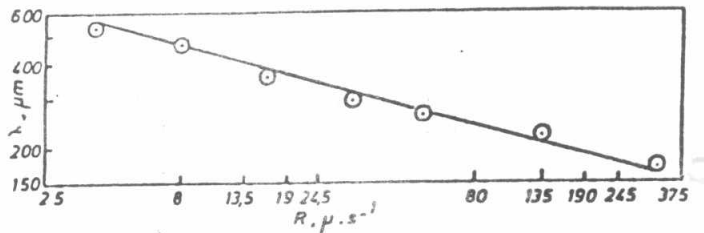


Figure 6. Primary arm spacing, λ_1 , as a function of growth rate, R , temperature gradient, G_L , is constant = 130 K.cm^{-1} , in low alloyed Mn-Ni steel (B).

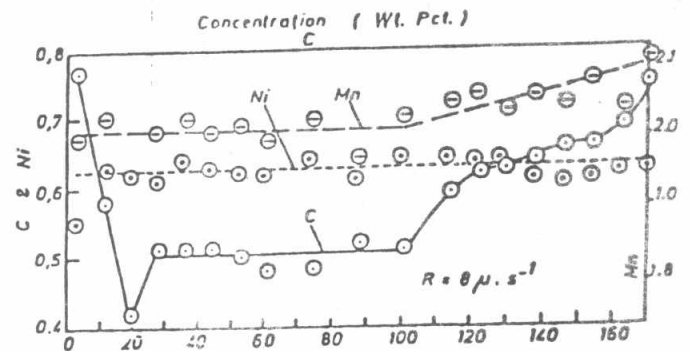


Figure 7. C, Ni and Mn distribution along longitudinal specimens of unidirectionally solidified low alloyed Mn-Ni steel (B). $G_L = 130 \text{ K.cm}^{-1}$, $R = 30 \text{ mm.h}^{-1}$.



From the above results, the dependence of the dendritic morphology on the solidification parameters, R and G , is quite clear. The influence of composition on the dendrite arm spacings is clear for the influence of carbon content. Comparison between results obtained for low carbon steels (W) and (X) and other steels with higher carbon, shows that λ_1 did not change with C% keeping R and G_L constant. The phenomenon occurring at the dendrite tip which controls primary arms seems to be only affected by R and G_L and not by the composition.^(5,7) On the other hand, λ_2 seems to be greatly dependent on the composition. From the present results, λ_2 shows a decrease as C% increases.

Macrosegregation

The distribution of main elements were determined along the directionally solidified castings, as shown in Fig.7 for the low alloyed Mn-Ni steel (B). Generally, while either positively or negatively segregated zones were observed at the lower end of the casting adjacent to the initial interface, terminal enrichment zone was always observed. The central part of the sample exhibited constant concentration distribution. This behavior is observed for all types of steel investigated. Carbon is the most segregating element. Mn and Cr show only relatively slight terminal enrichment. However, Ni shows almost constant concentration along the casting indicating no segregation.

An accurate explanation of the initial enrichment zone is difficult from the present results. However, this behavior has been⁽⁵⁾ attributed to the time interval during which the sample is liquid before it starts to solidify. Some solute diffuses out of the heterogeneous zone during this time. The terminal positive segregation is well known.^(1,2)

It is to be mentioned that the specimens cut from the casting for microstructure examination were taken from the central part where constant distribution of the elements exists.

Mechanical Properties

Some preliminary results on tensile properties of directionally



Table:2 : Values of the exponents in equations (1), (2) and (3) relating dendrite arm spacings in steels investigated with solidification parameters (Ref: 5-7).

Steel	n_1	n_2	n_3	m_1	m_2	m_3
(A)	0.27	--	--	0.47	0.36	--
(B)	0.29	--	--	--	--	--
(C)	0.19	0.57	--	0.39	0.36	--
(D)	0.17	0.41	--	0.36	0.37	--
(E)	0.25	0.41	0.34	0.31	0.37	0.43
(W)	0.27	--	--	0.38	0.46	--
(X)	0.27	--	--	0.47	0.46	--

Table:3 : Preliminary tensile test results obtained for low - alloyed Mn-Ni steel (B) - unidirectionally solidified compared with those obtained for similar material in forged condition.

Tensile Property	Unidirectionally Solidified		Forged
	$\bar{G} = 130 \text{ K.cm}^{-1}$ $R = 30 \text{ mm.h}^{-1}$ $\lambda_1 = 0.450 \text{ mm}$	$R = 200 \text{ mm.h}^{-1}$ $\lambda_1 = 0.25 \text{ mm}$	
0.2 Proof Strength	1120	563	536
Ultimate Strength	1226	1214	1066
Fracture Strength	1531	1264	1212
Fracture Elongation%	6	6	5.8
Fracture Reduction in Area%	25	12	12

Strength Values in N.mm^{-2} .



solidified low alloyed Mn-Ni steel (B) in the heat flow direction are given in table:3, together with results obtained for the same material but in forged condition. The tensile specimen of DS-casting was taken from the central part where a constant concentration exists. The forged specimen was subjected to a heat treatment process prior to tensile testing in order to get similar volume fraction of the phases as in the DS-specimen.

Generally, the DS-specimens show better strength and ductility than the forged ones. This is remarkable for specimens solidified at slow growth rates where rod-like aligned dendrites are formed. In this case, their tensile properties in comparison with the forged ones are: 2 times in proof strength, 1.15 times in ultimate tensile strength, 1.26 in fracture strength and 2 times in fracture reduction in area. At high growth rates and inspite of the finer dendrite arm spacing obtained, strength and ductility values were almost similar to those of forged specimens. The formation of secondary and tertiary arms at high growth rates, caused reduction in the properties in comparison with those of the aligned structure. More discussion is given elsewhere.⁽⁶⁾

STIR OR RHEO-CASTING

Materials and Experimental Procedures

Two different steels were used: carbon and stainless steels whose composition, liquidus and solidus temperatures, determined by differential thermal analysis, are given in table:4.

A batch type rheocaster, shown in Fig. 8, was designed to produce steel castings with 140 mm in diameter and 200 mm long. It consists of vacuum induction furnace to which a stirring device is attached. The stirrer was made of two crossed rods of Mo-Zr-oxide cermet attached to the main spindle of a portable drill. Precautions were taken so that heat loss, during rheocasting, are greatly minimized.⁽²⁰⁾ Rheocasting was achieved by starting the agitation at a temperature above the liquidus (100°C), using a speed of 600 rpm, then continuing it while the alloy is cooli-



Table:4 : Composition and liquidus and solidus temperatures of rheocast steels.

Steel	C%	Mn%	Si%	Cr%	Ni%	Mo%	T _L , °C	T _S , °C
Carbon Steel	1.0	1.0	--	--	--	--	1448	1358
Stainless Steel 440A	0.7	1.0	1.0	17	2	0.75	1510	1370

Table:5 : Composition determined in three positions of some rheocast stainless steel castings (Ref: 20).

T*, K	Position**	C%	Mn%	Si%	Cr%	Ni%	Mo%
15	1	0.67	0.94	0.72	17.1	2.03	0.96
	2	0.64	0.91	0.70	17.1	2.02	0.95
	3	0.65	0.91	0.72	17.3	2.03	0.94
65	1	0.71	0.75	0.77	16.5	2.07	0.90
	2	0.74	0.77	0.77	16.5	2.09	0.94
	3	0.72	0.75	0.75	16.4	2.09	0.90

* Temperature difference below the liquidus.

** 1) near casting periphery, 2) in the middle between periphery and centerline, and 3) casting centerline.



6

ng at the natural furnace cooling rate. When the selected temperature between liquidus and solidus is reached, isothermal stirring is kept for 12 minutes, then the slurry is poured immediately before being viscous.

Soundness

Generally, better surface quality was observed for the RC casting. RC castings exhibited good soundness and no cold shuts. Piping and centerline shrinkage, generally found in CC, are completely absent in RC. This is attributed to the better mass feeding⁽¹²⁾ flow of liquid and solid to feed solidification shrinkage, and to the agitation before pouring. Agitation postpones the formation of a continuous network and leaves the remaining liquid free to move and to counteract hot cracking tendency.⁽²¹⁾

Microstructure and Interparticle Spacing

In general, the microstructure of the RC steels is found to be homogeneous throughout the casting, which is not the case in CC. Typical RC structure⁽²⁰⁾ is presented in Fig. 9, where it is noticed that the conventional dendritic morphology has disappeared. The structure is composed of rounded primary particles formed during stirring, embedded in a matrix with fine structure (quenched remaining liquid). Similar structure has been also observed for different alloys.⁽¹¹⁻¹⁹⁾

A model for the formation of primary particles in RC alloys has been developed.⁽¹⁷⁾ The model is based on microstructural observations obtained by quenching specimens at different stages of the process. According to this model, the primary particle is first in the form of rosette which is then subjected to a fragmentation mechanism and therefore is breaking into several small rounded particles.

The interparticle spacing, λ , in RC, and the primary dendrite arm spacing, λ_1 in CC, are plotted⁽²⁰⁾ vs. distance from casting centerline in Fig. 10. λ of the RC is constant throughout the casting and falls between the maximum and minimum λ_1 values of CC.

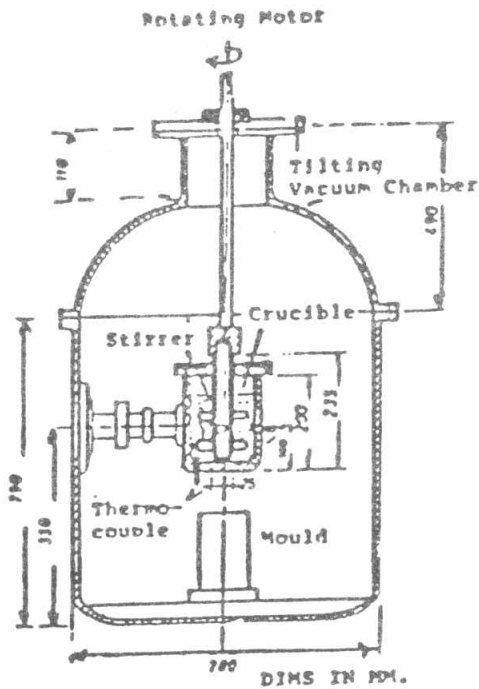


Figure 8. Apparatus used for rheocasting of steel.

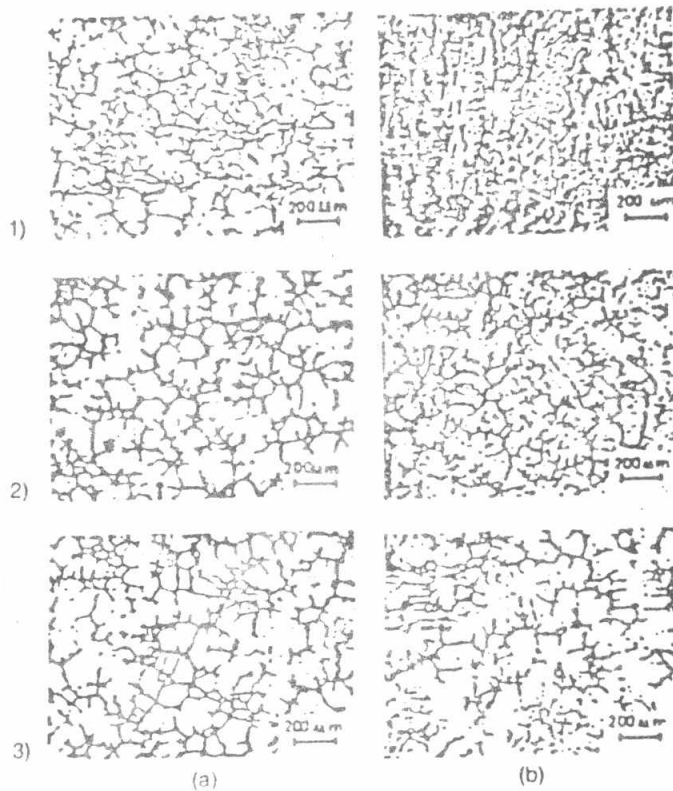


Figure 9. Typical microstructures at different positions of rheocast (a) and conventionally cast (b) stainless steel:

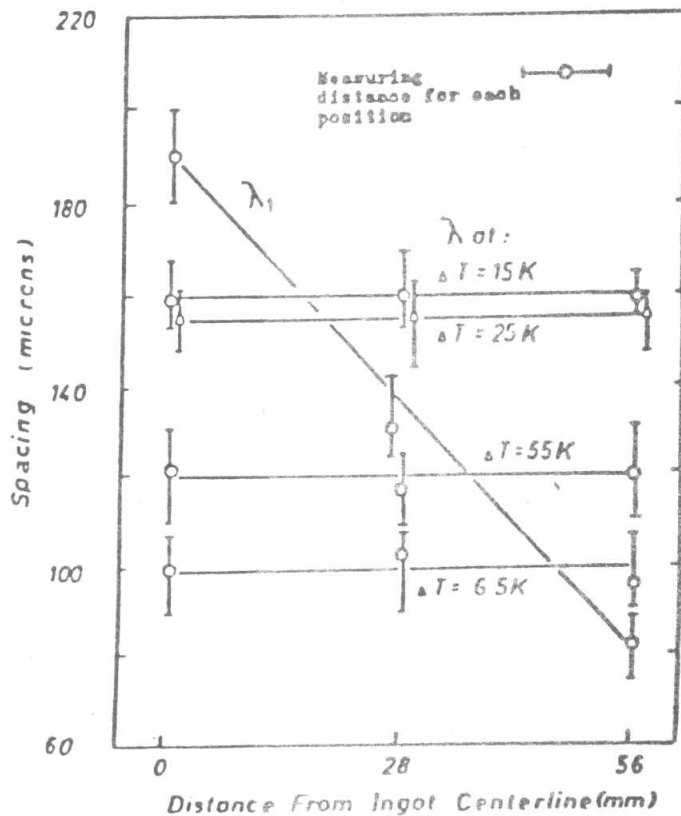


Figure 10. Particle spacing, λ , (RC) and primary arm spacing, λ_1 , (CC) of stainless steel castings as a function of distance

Fig. 10 also shows that, with lowering the RC temperature, λ decreases. On the otherhand, the volume fraction of the primary particles increases, i.e. a larger number of primary particles is formed. The particle shape is also affected by the RC temperature, since more rounded particles are formed at higher temperatures. This behavior is discussed elsewhere.⁽²⁰⁾

Segregation

Macrosegregation was determined for both RC and CC castings at different positions (periphery, centerline and in between) as shown in table:5. A large degree of chemical homogeneity is achieved in RC castings.

Microsegregation examined by microprobe analysis across primary particles is shown in Fig.11. A flat concentration profile for different elements is obtained, similar to other work on different alloys.^(13,15,16,18,22)

Mechanical Properties

Tensile tests were made on RC and CC stainless steel castings taken from different positions from periphery to centerline. In the CC material, the tensile strength, ductility and hardness, Fig.12, are found to decrease across the casting from periphery to centerline due to the increase in the dendrite arm spacing caused by the decrease of cooling rate from periphery to centerline. The RC steel shows uniform properties across the casting. The present results do not show any variation of the mechanical properties with RC temperature or interparticle spacing and volume fraction of primary solid within the range considered as shown in Fig.12. It is also found that tensile and hardness values of RC material fall between the maximum and minimum values measured for the CC material. In a word, the homogeneity in the structure and composition is reflected on the mechanical properties of the RC steel.

Compressive properties measured for the RC structure are also homogeneous across the casting. Interesting behavior is observed in this type of casting. Its compressive strength and ductility

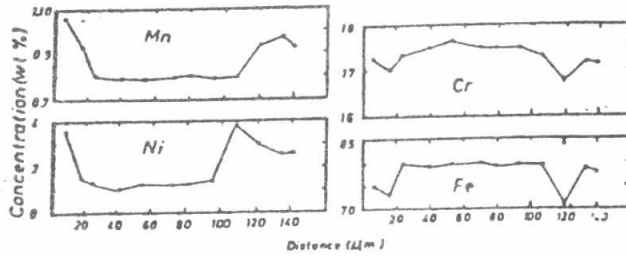


Figure 11. Distribution of Mn, Ni, Cr and Fe across a primary particle in rheocast stainless steel.

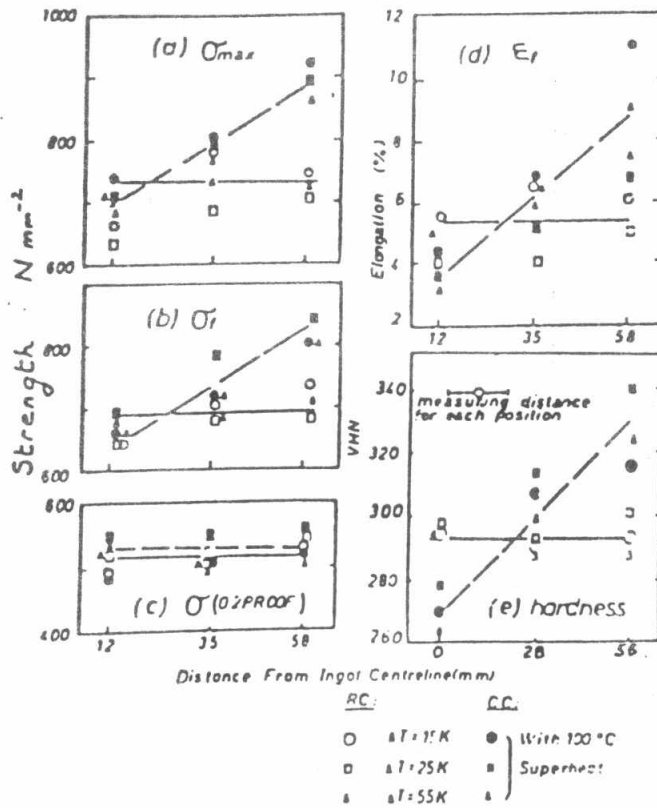


Figure 12. Tensile properties:



are found to be several times its tensile ones. The ultimate compressive strength measured was 7 times the tensile and the malleability (ductility in compression) was about 20 times the tensile ductility. The CC castings gave compressive properties not more than 3 times their tensile ones. More details about these results are found in another paper.⁽²⁰⁾ Similar behavior is also found for RC- Al-Cu alloys.^(18,23)

Conclusions

Unidirectional solidification and rheocasting of steel produce novel types of structure which can be controlled by the process solidification parameters. In the first process, aligned dendrites with rod-like shape can be formed as the temperature gradient / growth rate ratio increases. Such type of composite-like structure gave tensile properties in the axial direction even higher than that of the forged ones of the same material. In the case of rheocasting, rounded primary particles - homogeneous across the casting are obtained with lack of porosity, micro and macro-segregation. Therefore, homogeneous mechanical properties were obtained across the casting. The compressive properties in rheocastings were found to be several times their tensile ones.

REFERENCES

1. M. C. Flemings, Solidification Processing, Mc Graw-Hill Book Company, Inc., New York, 1974.
2. W. Kurz and D. J. Fisher, Fundamentals of Solidification, Trans. Tech. Publications Company, 1984.
3. N. A. El-Mahallawy and M. A. Taha, " Developments in Casting Processes for Improving Quality ", Second Int. Conf. on Prod. Eng., Design and Control, Alexandria University, Egypt, Dec. 1983.
4. M. A. Taha, N. A. El-Mahallawy, M. Abdel-Reihim and W. Reif, " Structural Developments in Solidified Alloys ", Z. Metall, Metall-Verlag GmbH, Berlin / Heidelberg, Heft 8, August 1983, P. 788 - 793.
5. M. A. Taha, H. Jacobi, N. Imaganbai and K. Schwerdtfeger, " Dendrite Morphology of Several Steady State Unidirectionally Solidified Iron Base Alloys ", Met. Trans. A, v. 13A, 1982, p. 2131 - 2141.
6. M. A. Taha, " Structure and Properties of Low Alloy Mn-Ni Steel with Controlled Solidification Structure ", to be published.
7. M. A. Taha, " Influence of Solidification Parameters on Dendrite Arm Spacings in Low Carbon Steels ", to be published.
8. W. Kurz and P. R. Sahm, " Gerichtet erstarrte eutektische Werkstoffe ", Springer-Verlag, Berlin, 1975.
9. N. A. El-Mahallawy, M. H. Abdel-Latif and M. A. Taha, " Microstructure of In-Situ Composites ", Z. Werkstofftechnik, 14, 1983, p. 115 - 119.
10. M. H. Abdel-Latif, N. A. El-Mahallawy and M. A. Taha, " Mechanical Properties of In-Situ Composites ", Z. Werkstofftech., 16, 1985, p. 116 - 121.
11. N. A. El-Mahallawy and M. A. Taha, " Rheocasting: Structure and Properties ", Current Advances in Mechanical Design and Production, Proc. 2nd Int. Cairo University MDP Conf.. 1982, p. 775 - 782.
12. D. B. Spencer, R. Mehrabian and M. C. Flemings, " Rheological



- Behavior of Sn-15 pct Pb in Crystallization Range ", Met. Trans., 3, 1972, p. 1925 - 1932.
13. A. Vogel, D. Doherty and B. Cantor, " Stir-Cast Microstructure and Slow Crack Growth ", Solidification and Casting of Metals, Metals Soc., London, 1978.
 14. S. D. E. Ramata, G. J. Abbaschian, and R. Mehrabian, " Structure of Partially Solid Alloys ", Met. Trans., 9B, 1978, p. 241 - 245.
 15. K. P. Young, R. G. Riek and M. C. Flemings, " Structures and Properties of Thixocast Steels", Solidification and Casting of Metals, Metals Soc., London, 1978.
 16. A. Assar, N. A. El-Mahallawy and M. A. Taha, " Influence of Rheocasting Variables on Structure and Porosity in Stir-Casting Al-Cu Alloys ", Metals Technology, v.9, 1982, p. 165 -169.
 17. M. A. Taha and N. A. El-Mahallawy, " Effect of Stirring of Partially Solidified Alloys (Rheocasting) on Their Structure and Properties ", Paper No. 15, 46th Int. Foundry Congress, Madrid, 1979.
 18. A. Assar, " Influence of Processing Variables in Alloy Rheocasting on Microstructure and Mechanical Properties ", M. Sc. Thesis, Faculty of Engineering, Ain-Shams University, Cairo - Egypt, 1981.
 19. A. Assar, N. A. El-Mahallawy and M. A. Taha, " Fluidity of Stir-Cast Al-10wt% Cu Alloy ", Aluminium, 12, 1981, p. 807 - 810.
 20. M. A. Taha and N. A. El-Mahallawy, " Structure and Mechanical Properties of Steel Produced by Rheocasting ", Proc. 3rd Int. Conf. on Mechanical Behaviour of Materials (ICM-3), Cambridge, U. K., v. 2, 1979, p. 537 - 546.
 21. S. A. Metz and M. C. Flemings, " A Fundamental Study of Hot Tearing ", AFS Trans., 78, 1970, p. 453 - 460.
 22. A. M. Assar, " Casting of Semi-Solid Alloys ", Ph.D. Thesis, Faculty of Engineering, Ain-Shams University, Cairo - Egypt, 1985.

MP-10	134
-------	-----



SECOND A.M.E. CONFERENCE
6 - 8 May 1986 , Cairo

23. N. A. El-Mahallawy, N. A. Fathalla and M. A. Taha, " Structure and Mechanical Properties of Al - Cu Alloys Produced by Rheocasting ", Proc. 4th Int. Conf. on Mechanical Behaviour of Materials (ICM-4), Stockholm, Sweden, v.2, 1983.